Biaxial Nematic Phase of Crank-like Bis(β-diketonato)copper(II) Complexes Established by X-ray Diffraction and Z-value Calculations

Yoriko Kanai, [a] Hajime Akimoto[a] and Kazuchika Ohta*[a]

[a] Smart Material Science and Technology, Interdisciplinary Graduate School of Science and Technology, Shinshu University, 1-15-1 Tokida, Ueda, 386-8567, Japan. Fax: 81-268-21-5492; Tel: 81-268-21-5492; E-mail: ko52517@shinshu-u.ac.jp

Abstract

We have synthesized a series of six novel bis(β-diketonate)copper (II) complexes, **1a**, **1b**, **2a**, **2b**, **3a** and **3b**, substituted by two bulky substituents in the short molecular axis direction to investigate their mesomorphism. The *m,p,m'*-trimethoxylphenyl-substituted derivatives, **2a** and **2b**, and the *m,p*-dimethoxylphenyl-substituted derivatives, **3a** and **3b**, did not show mesomorphism, whereas each of the *p*-methoxyphenyl-substituted derivatives **1a** and **1b** only showed a nematic phase, which was revealed from polarizing microscopic observations. We established from X-ray diffraction and Z-value calculations that each of the crank-like derivatives **1a** and **1b** forms a rectangular parallelepiped dimer and shows a biaxial nematic phase.

Key words: Biaxial nematic phase, bis(ß-diketonato)copper(II) complexes, metallomesogen, X-ray diffraction, Z-value calculations

Short title: Biaxial nematic phase of ß-diketonato copper complexes

I. INTRODUCTION

Nowadays, high-definition flat-panel televisions spread world-widely and liquid crystal display television is shared more than 90% in the flat-panel televisions [1]. Liquid crystal display has great advantages of low power consumption and long life, but it has disadvantages of narrow viewing angle and slower response to the electric field changes [2]. The former disadvantage was greatly improved by the innovation of Wide View film [3] using discotic liquid crystalline polymer in 1995. The latter disadvantage has been tried to resolve and the remedies have been proposed by many research groups. However, there have not yet been the practical ways. Among the proposed remedies, application of a biaxial nematic phase is the most promising to show fast response [4-6]. Therefore, we focus on novel molecular structures inducing a biaxial nematic phase in this study.

As illustrated in Fig. 1, the nematic liquid phases are broadly categorized into two states: (A) uniaxial nematic phase and (B) biaxial nematic phase. In the uniaxial nematic phases of

both rod-like and disk-like molecules, director vectors are aligned along the Z axis direction accompanied by free rotation of molecules in the XY plane, as illustrated in Fig.1 A. Therefore, the composition vector of the refractive indexes n_x and n_y compensate to be zero by free rotation and the vector of the refractive index n_z only remains. It results in uniaxiality. On the other hand, in the biaxial nematic phase of board-like molecules, the free rotations are prohibited around each of the X, Y and Z axes and the board-like molecules only slip in two directions, as illustrated in Fig. 1 B. Therefore, both the composition vector of the refractive indexes n_x and n_y, and the vector of the refractive index n_z remain. It results in biaxiality.

When a uniaxial nematic phase of rod-like molecules is used (Fig. 2 A(a)), the orientation change should require a large movement of the rod-like molecules from parallel to perpendicular arrangement between two glass plates. It is relatively time-consuming, so that the response speed becomes slow. On the other hand, when a biaxial nematic phase of board-like molecules is used (Fig. 2A(b)), the orientation change only requires a small angle change of face around Z axis of the board-like molecules. It is so easy that the response speed becomes much faster. As mentioned above, the biaxiality of nematogens can be induced when the free rotations are prohibited around each of the X, Y and Z axes of board-like molecules. If this condition can be achieved, the other molecular shapes can be also employed instead of the board-like molecules to show the biaxial nematic phase. As illustrated in Fig. 2B(c), banana-shaped biaxial nematogens has been extensively studied [7-9]. However, the

banana-shaped nematogens impose severe restrictions on the bending angle of the molecule to show a biaxial nematic phase. Therefore, it is not easy to obtain the biaxial nematic phase and expand the temperature range by chemically modifying the molecular structures. Accordingly, we have chosen a novel shape of crank-like molecule illustrated in Fig. 2B(d). In this study, we have employed crank-like bis(ß-diketonato)copper(II) complexes, which derivatives can be easily synthesized and modified.

The first biaxial nematogen based on bis(ß-diketonato)copper(II) complexes (Fig. 3A), which were substituted by two short *p*-alkylpnehyl or *p*-alkoxyphenyl (R_2) groups in the short molecular axis direction and two *n*-decyl (R_1) groups in the long molecular axis direction, were reported by Chandrasekhar *et al.* in 1987-1990 [10-12]. However, the biaxiality of these bis(ß-diketonato)copper(II) complexes was not accepted by the other research groups [13]. Therefore, the biaxiality has been still in dispute. In 1994, we also synthesized a novel series of nematogens (Fig. 3B) based on bis(ß-diketonato)copper(II) complex substituted by two ethyl (R_2) groups in the short molecular axis direction and two *n*-alkoxy (R_1O) groups in the long molecular axis direction. Contrary to our expectation, their mesophases were established as an optically positive uniaxial nematic phase, although they showed the same zig-zag disclination as the biaxial nematic phase of Chandrasekhar *et al.* [11]. Thus, the biaxiality of nematogens based on bis(ß-diketonato)copper(II) complex of Chandrasekhar *et al.* has remained as an open question for past two decades.

Recently we think that the uniaxiality of the nematogens (Fig. 3B) may be attributed to inadequate inhibition of the rotation around the long molecular axis by the ethyl (R_2) groups in the short molecular axis direction. Therefore, if the rotation around the long molecular axis would be adequately inhibited by bulkier R_2 groups in the short molecular axis direction, we could obtain biaxial nematogens based on the bis(ß-diketonato)copper(II) complex. Accordingly, in this study, we have employed three different bulkier substituents, *p*-methoxyphenyl, *m,p*-dimethoxylphenyl and *m,p,m'*-trimethoxylphenyl (Scheme 1), to induce biaxiality. As the results, the *m,p*-derivatives (**2**) and the *m,p,m'*-derivatives (**3**) are crystalline, whereas the *p*-derivatives (**1**) only show biaxial nematic phase which could be unambiguously established at the first time from temperature-dependent small angle X-ray diffraction mesophase structure analysis and the Z-value calculation [14]. To our best knowledge, it is the first time that biaxiality of nematic phases was established by using the Z-value calculations for two different models of cylinder and rectangular parallelepiped. We wish to report here the very interesting relationship between bulkiness of the substituent in the short molecular axis direction and appearance of biaxial nematic phase.

II. EXPERIMENTAL

II-1 Synthesis

Scheme 1 shows the synthetic route for a novel series of bis(ß-diketonato)copper(II) complexes,

1, **2** and **3**, which are substituted by *p*-methoxyphenyl [$(X_1,X_2,X_3)=(H,CH_3O,H)$], *m,p*-dimethoxylphenyl [$(X_1,X_2,X_3)=(CH_3O,CH_3O,H)$] and *m,p,m'*-trimethoxylphenyl [$(X_1,X_2,X_3)=(CH_3O,CH_3O,CH_3O)$] groups in the short molecular axis direction, respectively. All the starting materials were commercially available: *p*-hydroxybiphenyl (Wako Pure Chemical Industries), methyl *p*-methoxy benzoate (Tokyo Chemical Industry), methyl *m,p*-dimethoxy benzoate (Kanto Chemical), and methyl *m,p,m'*-trimethoxy benzoate (Wako Pure Chemical Industries). The target complexes were prepared by the methods reported by Gray *et al.* [15] and our previously reported methods [16-18]. The detailed procedures are described only for the representative derivatives **1a**~**7a** for n = 12 (**a**), in the followings. Since the derivatives **1b**~**7b** for n = 14 (**b**) could be synthesized in the same manner, these physical property data are only described here.

4-Dodecyloxybiphenyl(7a)

Into a 200ml of three-necked flask, hydroxybiphenyl (10.0 g, 58.8 mmol), potassium carbonate (16.2 g, 0.118 mol) and freshly distilled dry DMF (30 ml) were added and stirred. To the mixture, bromododecane (17.6 g, 70.5 mmol) was added, and it was refluxed for 1 hour. After cooling to rt, the reaction mixture was extracted with chloroform and washed with water. The organic layer was dried over sodium sulfate overnight. The organic solvent was evaporated under reduced pressure. The residue was dried under vacuum and recrystallized from ethanol

to afford 18.5 g of white crystals.

Yield: 93% Melting point: 80.9 ~81.5 ℃

IR(KBr): ν, cm^{-1} 2920.17, 2851.09(-CH_2-)

^{1}H-NMR(TMS / $CDCl_3$, ppm); δ = 0.88(t, J=6.8Hz, 3H, CH_3), 1.27(brs, 16H, C*H*$_2C_2H_5$), 1.75~1.84(m, 2H, $C_{10}H_{21}$C*H*$_2$), 3.99 (t, J=6.5, 2H, $C_{11}H_{23}$C*H*$_3$), 6.96(d, 2H, J=8.8 arom), 7.26~7.32(m, 1H, arom), 7.40(t, J=7.7, 2H, arom), 7.48~7.57(m, 4H, arom).

4-Tetradecyloxybiphenyl(7b)

Yield: 93% Melting point: 85.5~85.6 ℃

IR(KBr): ν, cm^{-1} 2935.65, 2850.66(-CH_2-)

^{1}H-NMR(TMS / $CDCl_3$, ppm); δ = 0.88(t, J=7.3Hz, 3H, C*H*$_3$), 1.43~1.50(m, 2H, CH_3C*H*$_2$), 1.24~1.38(m, 16H, $C_2H_5C_8$*H*$_{16}$), 1.76~1.85(m, 2H, $C_{10}H_{21}$C*H*$_2$), 2.62(s, 3H, COC*H*$_3$), 4.00 (t, J=6.6, 2H, $C_{11}H_{23}$C*H*$_3$), 6.99(d, J=4.4, 2H, arom), 7.56(d, J=4.4, 2H, arom), 7.64(d, J=4.3, 2H, arom), 8.00(d, 2H, arom).

4-Dodecyloxy-4'-acethylbiphenyl(8a)

Into a 200 ml three-necked flask, 4-dodecyloxybiphenyl (8.00 g, 23.6 mmol) and 30 ml of dry dichloromethane were poured and stirred in an ice-water bath under nitrogen atmosphere. To the mixture, powdered aluminum chloride (4.72 g, 35.4 mmol) was added and then acetyl chloride (2.78 g 35.4 mmol) was slowly added dropwise. The reaction mixture was kept at 0 ℃ for 2 hours, and then refluxed for 1 hour. After cooling to rt, the reaction mixture was

poured into an ice water containing a 10% HCl aqueous solution. After neutralization of the solution with sodium bicarbonate, it was extracted with chloroform and washed with water. The organic layer was dried over Na_2SO_4 overnight. The organic solvent was evaporated under reduced pressure. The residue was dried under vacuum and recrystallized from ethanol and then isopropyl alcohol to afford 3.64 g of pale yellow crystals.

Yield: 41%. Melting point: 128.0~128.7 ℃.

IR(KBr): ν, cm^{-1} 1680.01(aromatic ketone).

4-Tetradecyloxy-4'-acethylbiphenyl(8b)

Yield: 29%. Melting point: 124.2 ~125.0 ℃.

IR(KBr): ν, cm^{-1} 1679.56(aromatic ketone)

1-(4'-Dodecyloxybiphenyl)-3-(4-methoxyphenyl) propane-1, 3-dione(4a)

Into a 100 ml of three-necked flask, a mixture of NaH (60% assay: 0.24 g in mineral oil, 6.0 mmol) washed with dry distilled n-hexane, and 10 ml of dry freshly distilled THF were added and stirred under nitrogen atmosphere. To the mixture, 4-dodecyloxy-4'-acethylbiphenyl (**8a**: 0.61 g, 1.6 mmol) was added and then a solution of methyl 4-methoxybenzoate (1.3 g, 8.0 mmol) dissolved in 10 ml of dry THF was added dropwise. The reaction mixture was refluxed for 13 hours. It was cooled with ice-water bath and 5.0ml of 10% HCl aqueous solution was added to quench the reaction. It was extracted with chloroform and washed with water. The organic layer was dried over Na_2SO_4. The solvent was evaporated under reduced pressure.

The residue was dried under vacuum and recrystallized from dichloromethane to afford 0.67 g of slightly reddish pale yellow crystals.

Yield: 80%. Melting points: 140.8 ℃, 146.7 ℃ (keto-type and enol type, respectively).

^{1}H-NMR(TMS / $CDCl_3$, ppm); δ = 0.88(t, J=6.6Hz, 3H, $CH_3C_9H_{18}CH_2CH_2O$), 1.21~1.56(m, 18H, $CH_3C_9H_{18}CH_2CH_2O$), 1.76~1.86 (m, 2H, $CH_3C_9H_{18}CH_2CH_2O$), 3.89 (s, 3H, OCH_3), 4.01(t, 2H, J=6.6 $CH_3C_9H_{18}CH_2CH_2O$), 6.96~7.02(m: 5H, COCHCOH + arom), 7.55~7.62(m, 2H, arom), 7.64~7.70(m, 2H, arom), 7.97~8.07(m,4H, arom).

1-(4'-Tetradecyloxybiphenyl)-3-(4-methoxyphenyl) propane-1, 3-dione(4b)

Yield: 54%. Melting point: 148.5 ℃.

1-(4'-Dodecyloxybiphenyl)-3-(3, 4-dimethoxyphenyl) propane-1, 3-dione (5a)

Into a 100 ml three-necked flask, a mixture of NaH(60% assay: 0. 28 g in mineral oil, 7.0 mmol) washed with dry distilled n-hexane, and 10 ml of dry freshly distilled THF were added and stirred under nitrogen atmosphere. To the mixture, 4-dodecyloxy-4'-acethylbiphenyl(**8a**: 0.89 g, 2.3 mmol) and then a solution of methyl 3,4-dimethoxybenzoate (2.3 g, 11.7 mmol) dissolved in 12 ml of dry THF were added dropwise. The reaction mixture was refluxed for 17 hours. It was cooled with ice-water bath and 5.0ml of 10% HCl aqueous solution was added to quench the reaction. It was extracted with chloroform and washed with water. The organic layer was dried over Na_2SO_4. The solvent was evaporated under reduced pressure. The residue was dried under vacuum and purified by recrystallization from ethanol and column

chromatography (silica gel 60 g, CH_2Cl_2 : ethyl acetate = 98 : 2; Rf = 0.57) to afford 0.28 g of pale yellow crystals.

Yield: 23%. Melting point: 105.1 ℃, clearing point: 116.3 ℃.

^{1}H-NMR(TMS / $CDCl_3$, ppm); δ = 0.84(t, J=6.6Hz, 3H, $CH_3C_9H_{18}CH_2CH_2O$), 1.21~1.52(m, 18H, $CH_3C_9H_{18}CH_2CH_2O$), 1.76~1.86(m, 2H, $CH_3C_9H_{18}CH_2CH_2O$), 3.91~4.04(m, 8H, $CH_3C_9H_{18}CH_2CH_2O + OCH_3$), 6.95~7.00(m: 4H, COCHCOH + arom), 7.54~7.70(m, 6H, arom), 8.02(d, 2H, J=11.37, arom).

1-(4'-Tetradecyloxybiphenyl)-3-(3, 4-dimethoxyphenyl) propane-1, 3-dione (5b)

Yield: 13%. Melting point: 87.0 ℃, clearing point: 99.1 ℃.

1-(4'-Dodecyloxybiphenyl)-3-(3, 4, 5-trimethoxyphenyl)-propane-1, 3-dione (6a)

Into a 100 ml three-necked flask, a mixture of NaH (60% assay: 0.214 g in mineral oil, 5.25 mmol) and 10 ml of dry distilled THF was added and stirred under nitrogen atmosphere. To the mixture, 4-dodecyloxy-4'-acethylbiphenyl (**8a**: 1.00 g, 2.63 mmol) and then methyl 3,4,5-trimethoxybenzoate (7.56 g, 13.2 mmol) dissolved in 20ml of dry THF were added dropwise. The reaction mixture was refluxed for 13 hours. It was cooled with ice-water bath and 5ml of 10% HCl aqueous solution was added to quench the reaction. It was extracted with chloroform and washed with water. The organic layer was dried over Na_2SO_4. The solvent evaporated under reduced pressure. The residue was dried under vacuum and purified by recrystallization from ethanol and column chromatography (silica gel 70 g, $CHCl_3$: n-hexane

= 7 : 3; Rf = 0.15). Finally, it was recrystallized again from acetone to afford 0.782 g of yellow crystals.

Yield: 52%. Melting point: 116.9 ℃.

^{1}H-NMR(TMS / $CDCl_3$, ppm); δ = 0.88(t, J=7.1Hz, 3H, C*H*$_3$C$_9$H$_{18}$CH$_2$CH$_2$O), 1.21~1.51(m, 18H, CH$_3$C$_9$*H*$_{18}$CH$_2$CH$_2$O), 1.77~1.86(m, 2H, CH$_3$C$_9$H$_{18}$C*H*$_2$CH$_2$O), 3.92~3.99(3 × s, 9H, OCH$_3$), 4.02(t, 2H, J=6.57, CH$_3$C$_9$H$_{18}$CH$_2$C*H*$_2$O), 6.80(s, 1H, COC*H*COH), 6.99(d, 2H, J=4.5, arom), 7.25(s, 2H, arom), 7.58(d, 2H, J=4.4, arom), 7.68(d, 2H, J=4.3, arom), 8.03(d, 2H, J=4.3, arom).

1-(4'-Tetradecyloxybiphenyl)-3-(3, 4, 5-trimethoxyphenyl)-propane-1, 3-dione (6b)

Yield: 67%. Melting point: 124.1 ~ 125.1 ℃.

Bis[1-(4'-dodecyloxybiphenyl)-3-(4-methoxyphenyl)propane-1,3-dionato]copper(II) (1a)

Into a 100 ml three-necked flask, 1-(4'-dodecyloxybiphenyl)-3-(4-methoxyphenyl) propane-1, 3-dione (**4a**: 0.20 g, 0.39 mmol), 20 ml of toluene and 15 ml of ethylene glycol were poured. The mixture was heated to 110 °C and stirred. After confirming that the diketone **4a** had been dissolved, 1.0 ml of KOH aqueous solution (0.10 mol/l) was added to the solution. Immediately after adding a solution of $CuCl_2$ (0.066 g, 0.49 mmol) in 5.0 ml ethanol to the solution, pale yellowish green solid formed. The oil bath was removed and stirring was continued for 30 minutes. To the reaction mixture at room temperature, 200 ml of ethanol and 50 ml of water were successively poured. The precipitated pale yellowish green crystals were collected by

filtration and washed with ethanol several times until the odor of toluene vanished. Furthermore, the crystals were washed with hot water and then hot ethanol. The residue was recrystallized twice from ethyl acetate to give 0.10 g of pale yellowish green crystals.

Yield: 25%. Melting point: 125.7 ℃, clearing point: 141.4 ℃.

Bis[1-(4'-tetradecyloxybiphenyl)-3-(4-methoxyphenyl)propane-1,3-dionato] copper(II) (1b)

Yield: 18%. Melting point: 159.2 ℃, clearing point: 173.5 ℃.

Bis[1-(4'-dodecyloxybiphenyl)-3-(3,4-dimethoxyphenyl)propane-1,3-dionato] copper(II) (2a)

Into a 100 ml three-necked flask, 1-(4'-dodecyloxybiphenyl)-3- (3, 4-dimethoxyphenyl) propane -1, 3-dione (**5a**: 0.14 g, 0.26 mmol) and 25 ml of ethanol were poured. The mixture was heated to 85 ℃ and stirred. After confirming that the diketone **5a** had been dissolved, to the solution were added 1ml of 25% NH_4OH aqueous solution and then a solution of $CuCl_2$ (0.046 g, 0.34 mmol) in 5 ml of ethanol, dropwise. After cooling to rt, the precipitated yellowish green solid was collected by filtration and washed with hot water and then hot ethanol. The residue was recrystallized from ethyl acetate to give 0.14 g of yellowish green crystals.

Yield: 54%. Melting point: 197.3 ℃.

Bis[1-(4'-tetradecyloxybiphenyl)-3-(3,4-dimethoxyphenyl)propane-1,3-dionato] copper(II) (2b)

Yield: 18%. Melting point: 184.5 ℃.

Bis[1-(4'-dodecyloxybiphenyl)-3-(3,4,5-trimethoxyphenyl) propane-1,3-dionato] copper(II) (3a)

Into a 100 ml three-necked flask, 1-(4'-dodecyloxybiphenyl)-3-(3,4,5-trimethoxy-phenyl)-propane-1,3-dione (**6a**: 0.29 g, 0.51 mmol) and 35 ml of ethanol were poured. The mixture was heated to 90℃ and stirred. After confirming that the diketone **6a** had been dissolved, to the solution were added 1ml of 25% NH_4OH aqueous solution (0.10 mol/l) and then a solution of $CuCl_2$ (0.085 g, 0.63 mmol) in 5 ml of ethanol, dropwise. After cooling to rt, the precipitated yellowish green solid was collected by filtration and washed with hot water and then hot ethanol. The residue was recrystallized from ethyl acetate to give 0.28 g of yellowish green crystals.

Yield: 45%. Melting point: 227.3 ℃.

Bis[1-(4'-tetradecyloxybiphenyl)-3-(3,4,5-trimethoxyphenyl) propane-1,3-dionato] copper(II) (3b)

Yield: 23%. Melting point: 212.1 ℃.

II-2 Measurements

The ^{1}H-NMR measurements were carried out by using ^{1}H-NMR (Bruker Ultrashield 400 M Hz). The elemental analyses were performed by using a Yanaco CHN CORDER MT-3. Table 1 lists up the elemental analysis data of the present bis(β-diketonato)copper(II) complexes (**1a**~**b**, **2a**~**b** and **3a**~**b**). Phase transition behavior of the present copper(II) complexes **1**~**3** and the corresponding ligands **4**~**6** was observed with polarizing optical microscope (Nikon ECLIPSE E600 POL) equipped with a Mettler

FP82HT hot stage and a Mettler FP-90 Central Processor, and a Shimadzu DSC-50 differential scanning calorimeter. The mesophases were identified by using a small angle X-ray diffractometer (Bruker Mac SAXS System) equipped with our developed temperature-variable sample holder adopted a Mettler FP82HT hot stage. The setups of the SAXS system and the temperature-variable sample holder are illustrated in Figs. 4 and 5, respectively. As can be seen from Fig. 4, the generated X-ray is bent by two convergence monochrometers to produce point X-ray beam (diameter = 1.0 mm). The point beam runs through holes of the temperature-variable sample holder. As illustrated in Fig. 5, into the temperature-variable sample holder of Mettler FP82HT hot stage, a glass plate (76 mm × 19 mm × 1.0 mm) having a hole (diameter = 1.5 mm) is inserted. The hole can be charged with a powder sample (*ca.* 1 mg). The measurable range is from 3.0 Å to 110 Å and the temperature range is from rt to 375 ℃. This SAXS system is available for all condensed phases including fluid nematic phase and isotropic liquid.

III. RESULTS AND DISCUSSION

III-1 Phase transition behavior

The phase transition temperatures were determined by using a polarizing optical microscope (POM) and a differential scanning calorimetry (DSC). In Table 2, is summarized the phase transition behavior of the bis(ß-diketonato)copper (II) complexes **1~3** and their

corresponding ligands **4~5**. As can be seen from this table, each of the copper complexes and the ligands is crystalline at rt.

When the crystal of *m,p,m'*-trimethoxylphenyl–subustituted ligand **6a** was heated from rt, it directly melted into isotropic liquid (I.L.) at 118.8 ℃ (IL). On the other hand, when the I.L. was cooled down, it transformed into a monotropic smectic A phase at 110.4 ℃ (see Photomicrograph [A] in Fig. 6). The homologous ligand **6b** showed no mesophase even in cooling stage. The corresponding copper(II) complexes **3a** and **3b** did not show mesomorphism. Each of the *m,p*-dimethoxylphenyl–substituted ligands **5a** and **5b** showed an enantiotropic smectic A phase (see Photomicrograph [B] in Fig. 6), whereas the corresponding *m,p*-dimethoxylphenyl-substituted copper(II) complexes **2a** and **2b** did not show mesopmorphism. No mesomorphism of the copper(II) complexes **2a~b** and **3a~b** may be attributed to the bulkier substituents of *m,p*-dimethoxylphenyl and *m,p,m'*-trimethoxylphenyl groups which prevent to sliding of the copper(II) complexes in any directions.

Although the *p*-methoxyphenyl-substituted ligand **4a** did not show mesomorphism, two different mps could be observed at 140.8 and 146.7 ℃ by POM. This ligand **4a** may exist as both keto and enol forms having different mps by tautomerization of the part of diketone.

Fig. 7 shows DSC thermograms of the ligands **4a**, **5a** and **6a**. As can be seen from Fig. 7[A], two endothermic peaks at their mps of 140.8 and 146.7 ℃ with almost the same intensities. On the other hand, ligand **5a** showed a big endothermic peak at 105.1 ℃ of the mp

accompanied with a small endothermic peak at a little bit lower temperature (Fig. 7[B]). Ligand **6a** showed only one peak at the mp (Fig. 7[C]). It is attributable to three electrodonating methoxy groups, which may originate 100% of enol form for the *m,p,m'*-trimethoxylphenyl-substitued ligand **6a**. The enol form percentage may decrease with decreasing the number of methoxy groups. Therefore, *m,p*-dimethoxylpheny-substituted ligand **5a** may give only a small percentage of keto form, and *p*-methoxyphenyl-substituted ligand **4a** may give a large amount of the keto form with equal amount of the enol form.

It is very interesting that the *p*-methoxyphenyl-substituted copper(II) complexes, **1a** and **1b**, only show mesomorphism among these copper complexes, **1~3**. As can be seen from Fig. 6[C], the copper complexes, **1a**, showed a Schlieren texture having two and/or four brushes which is a characteristic of nematic mesophase. Spontaneous fluidity and partial homeotropic alignment could be also observed. The homologous copper complex, **1b**, also gave the same Schlieren texture.

III-2 Temperature-variable small angle X-ray scattering (SAXS) studies

Figs. 4 and 5 illustrate the setups of our developed SAXS system and the temperature-variable sample holder, respectively. As described the details in the experimental section, this SAXS system is available for all condensed phases including fluid nematic phase and isotropic liquid. Therefore, we have measured various kinds of nematic phases by using this system. The X-ray diffraction patterns and the X-ray data of these

nematic phases are summarized in Fig. 8, Fig. 9 and Table 3.

First of all, we measured the X-ray diffraction (XRD) patterns of a well-known uniaxial nematogen of *p-n*-decyloxybenzoic acid. As can be seen from Fig. 8[A], the nematic phase at 133℃ gave two broad peaks at 2Θ = *ca.* 3° and *ca.* 20°, which correspond to the average distances, a(= 29.90 Å) and b(= 4.534 Å), in long and short molecular axis directions among the neighboring rod-like molecules, respectively (See Fig. 1[A](i)).

Hereupon, supposing a cylinder may have these two values, a(= 29.90 Å) and b(= 4.534 Å), the number of molecules contained in the cylinder should be integer. If the number is one, the cylinder sizes, a and b, correspond to the longitude (a) and diameter (b) of the rod-like molecule, respectively (See Fig. 1[A](i)). Therefore, we can estimate the number of molecules (Z) in the cylinder volume (V) from the following equations [14]:

$V = \pi \times (b/2)^2 \times a,$

$Z = \rho \times V \times N/M$

, where ρ, N, and M are an assumed density of the nematic phase (1.0 g/cm^3), Avogadro's number (6.02 ×10^{23}/mol) and molecular weight (g/mol), respectively.

$Z = 1.0\ (g/cm^3) \times (4.534\times10^{-8}\ (cm) / 2)^2 \times 29.90\times10^{-8}\ (cm) \times 6.02\times10^{23}(/mol) / 278.39\ (g/mol) = 1.04 \approx 1.0$

Thus, this Z value is not two but just one. The integer 1 means that *p-n*-decyloxybenzoic acid does not form dimer in the present nematic phase. Although we have long believed that

p-n-decyloxybenzoic acid should form dimer in the nematic phase, the Z value calculation apparently indicates that it does not form dimer in the nematic phase. Nevertheless, the uniaxiality of the nematic phase could be confirmed by this Z-value calculation for the cylinder model for a uniaxial nematic phase. Thus, the present XRD pattern of *p-n*-decyloxybenzoic acid is consistent with a uniaxial nematic (N_u) phase.

As can be seen from Fig. 8[B], the isotropic liquid (I.L.) at 152 ℃ also gave two broad peaks at 2Θ = *ca.* 3° and *ca.* 20°, but the intensity of the broad peak at 2Θ = *ca.* 3° is much weaker than that of the N_u phase. This means that the order in long axis direction lost in the I.L. much more than the N_u phase.

Next, we measured the XRD patterns of another nematogen of bis [1-(4'-dodecyloxybiphenyl)- 3-ethyl-propane-1,3-dionato]copper(II) (Fig. 3 [B]; n = 12) which mesophase had been well established as an optically positive uniaxial enantiotropic nematic phase [18]. As can be seen from Fig. 8[C], this copper complex at175 ℃ also gave two broad peaks at 2Θ = *ca.* 3° and *ca.* 20°, which correspond to the average distances, a(= 30.47 Å) and c(= 4.642 Å), among the neighboring board-like molecules, respectively (See Fig. 1[B](iii)). This copper complex is board-like, but the XRD pattern gave only two broad peaks which indicate that the mesophase is a uniaxial nematic (N_u) phase. It is consistent with our identification of the mesophase as a uniaxial nematic (N_u) phase from optical microscopic observations in our previous work [18]. Fig. 8[D] shows the XRD pattern of the I.L. at 215 ℃.

The intensity of the broad peak at 2Θ = *ca.* 3° is a little bit weaker than that of the N_u phase.

Finally, we measured the XRD patterns of the present novel nematogens, **1a** and **1b**. Fig. 9 [A] and [C] show the XRD patterns of the nematic phases of **1a** and **1b**, respectively. On the other hand, Fig. 9[B] and [D] show the XRD patterns of the I.L.s of **1a** and **1b**, respectively. The XRD patterns of these I.L.s in Fig. 9 [B] and [D] are the same as those in Fig. 8[B] and [D] of the previous nematogens, *p-n*-decyloxybenzoic acid and bis [1- (4'-dodecyloxybiphenyl)-3-ethyl-propane-1,3-dionato]copper(II). On the other hand, the XRD patterns of the present nematic phases in Fig. 9 [A] and [C] gave an additional peak b, which could not be seen in the XRD patterns in Fig. 8 [A] and [C] for the uniaxial nematic mesophases of the previous nematogens. The previous uniaxial nematic phases gave only two broad peaks a and b (See Fig. 8 [A] and [C]), whereas the present nematic mesophase of **1a** and **1b** gave three peaks, a, b and c, as can be seen from Fig. 9 [A] and [C]. The peaks a, b and c correspond to the average distances in X, Y and Z directions among the neighboring board-like molecules, respectively (See Fig. 1 [B](iii)). Appearance of these three peaks, a, b and c in the X-ray diffraction patterns in Fig. 9 [A] and [C] is an evidence of a biaxial nematic (N_b) phase [19]. Therefore, the present nematic mesophase of **1a** and **1b** can be consistently identified as a biaxial nematic (N_b) phase.

III-3 Proof of biaxiality from Z-value calculation

Hereupon, supposing an apparent rectangular parallelepiped unit cell may have these

three values, a, b and c, the number of molecules in the unit cell should be integer. If the number is one, the unit cell sizes a, b and c correspond to the longitude (a), wideness (b) and thickness (c) of the board-like molecule, respectively (See Fig. 1[B]). Therefore, we can estimate the number of molecules (Z) contained in a volume of a board-like molecule (V) from the following equations [14]:

$V = a \times b \times c$,

$Z = \rho \times V \times N/M$

, where ρ, N, and M are an assumed density of the nematic phase (1.0 g/cm^3), Avogadro's number (6.02 ×10^{23}/mol) and molecular weight (g/mol), respectively.

For the derivative **1a** (a = 35.64 Å, b = 21.34 Å, c = 4.64 Å),

$Z = 1.0\ (g/cm^3) \times \{35.64\times10^{-8}\ (cm) \times 21.34\times10^{-8}\ (cm) \times 4.64\times10^{-8}\ cm\} \times 6.02\times10^{23}(/mol) /$

$1091\ (g/mol) = 1.95 \approx 2.0$

Thus, this Z value is not one but just two. The integer two means that the crank-like derivative **1a** forms rectangular parallelepiped dimer in the present nematic phase. Nevertheless, the integer obtained from this Z-value calculation for the rectangular parallelepiped dimer model itself proved the biaxiality of the nematic phase.

For the derivative **1b** (a = 33.85 Å, b = 23.88 Å, c = 4.85 Å),

$Z = 1.0\ (g/cm^3) \times \{33.85\times10^{-8}\ (cm) \times 23.88\times10^{-8}\ (cm) \times 4.85\times10^{-8}\ cm\} \times 6.02\times10^{23}(/mol) /$

$1149\ (g/mol) = 2.05 \approx 2.1$

This Z value two means that the crank-like derivative **1b** also forms rectangular parallelepiped dimer in the nematic phase, and proved the biaxiality of the nematic phase, similarly to the homologous crank-like derivative **1a**.

Figure 10 illustrates a proposed dimer model for **1a** and **1b** in the N_b phase. As can be seen from this model, the free rotations may be prohibited around all the axis directions of the board-like molecules to originate the biaxial nematic phase.

IV. CONCLUSION

We have synthesized a series of six novel bis(β-diketonate)copper (II) complexes, **1a**, **1b**, **2a**, **2b**, **3a** and **3b**, substituted by two bulky substituents in the short molecular axis direction to investigate their mesomorphism. The *m,p,m'*-trimethoxylphenyl-substituted derivatives (**2a** and **2b**) and the *m,p*-dimethoxylphenyl-substituted derivatives (**3a** and **3b**) did not show mesomorphism, whereas the *p*-methoxyphenyl-substituted derivatives (**1a** and **1b**) only showed a biaxial nematic phase. Thus, the bulkier substituents in the short molecular axis direction may prevent the derivatives **2** and **3** from inducing mesomorphism, whereas the moderately bulky substituent *p*-methoxyphenyl group in the short molecular axis direction may induce the biaxial nematic phase for the derivative **1**. Thus, the substitution of bulky group in the short molecular axis direction can be a key point to induce the biaxial nematic phase. From X-ray diffraction studies and the Z-value calculations, we have established that

each of the crank-like derivatives **1a** and **1b** forms rectangular parallelepiped dimer and shows a biaxial nematic phase. To our best knowledge, it is the first time that biaxiality of nematic phases was established by using the Z-value calculations for two different models of cylinder and rectangular parallelepiped. We believe that this finding will be a good guideline to obtain new nematogens showing biaxiality.

REFERENCES

[1] See Figure 1 in http://www.displaysearch.com/cps/rde/xchg/displaysearch/hs.xsl/121023_global_tv_demand_expected_to_be_flat_in_2013.asp

[2] http://whatis.techtarget.com/definition/Flat-panel-TV-Guide

[3] Kawata, K. (2002). *The Chemical Record*, ***2***, 59.

[4] Tschierske, C. and Photinos, D. J. (2010). *J. Mater. Chem.*, ***20***, 4263.

[5] Freiser, M. J. (1970). *Phys. Rev. Lett.*, , ***24***, 1041.

[6] Straley, J. P. (1974). *Phys. Rev.*, ***A10***, 1881.

[7] Lehmann, M., Seltmann, J., Auer, A. A., Prochnowb, E., and Benedikt, U. (2010). *J. Mater. Chem.*, ***20***, 4263.

[8] Keith, C., Prehm, M., Panarin, Y. P., Vij, J. K., and Tschierske, C. (2010). *Chem. Commun.*, ***46***, 3702.

[9] Lee, S. K., Li, X., Kang, S., Tokita, M. and Watanabe, J. (2009). *J. Mater. Chem.*, ***19***, 4517.

[10] Chandrasekhar, S., Sadashiva, B. K., and Srikanta, B. S. (1987). *Mol. Cryst. Liq. Cryst.*, ***151***, 93.

[11] Chandrasekhar, S., Ratna, B. R., Sadashiva B. K., and Raja, V. N. (1988). *Mol. Cryst. Liq. Cryst.*, ***165***, 123.

[12] Chandrasekhar, S., Raja, V. N., and Sadashiva, B.K. (1990). *Mol. Cryst. Liq. Cryst. Lett.*, ***7***, 65.

[13] Luckhurst, G. R. (2001). *Thin Solid Films*, ***393***, 40.

[14] Ohta, K. (2013). *Dimensionality and Hierarchy of Liquid Crystalline Phases: X-ray Structural Analysis of the Dimensional Assemblies*, Shinshu University Institutional Repository, submitted on 11 May, 2013; http://hdl.handle.net/10091/17016; Ohta, K. (2007). *Identification of discotic mesophases by X-ray structure analysis*, in *Introduction to Experiments in Liquid Crystal Science (Ekisho Kagaku Jikken Nyumon [in Japanese])*, (Ed.) Japanese Liquid Crystal Society, Chapter 2-(3), pp. 11–21, Sigma Shuppan, Tokyo,; ISBN-13: 978-4915666490.

[15] Gray, G. W., Jones, B. and Marson, F. (1957). *J. Chem. Soc.*, 393.

[16] Ohta, K., Muroki, H., Hatada, K., Yamamoto, I., and Matsuzaki, K. (1985). *Mol. Cryst. Liq. Cryst.*, ***130***, 249.

[17] Ohta, K., Takenaka, O., Hasebe, H., Morizumi, Y., Fujimoto T., and Yamamoto, I. (1991). *Mol. Cryst. Liq. Cryst.*, ***195***, 103.

[18] Ohta, K., Akimoto, H., Fujimoto, T. and Yamamoto, I. (1994). *J. Mater. Chem.*, ***4***, 61.

[19] Praefcke, K., Gundogan, B. Singer, D., Demus, D., Diele, S., Pelzl, G., and Bakowsky, U. (1991). *Mol. Cryst. Liq. Cryst.*, ***198***, 393.

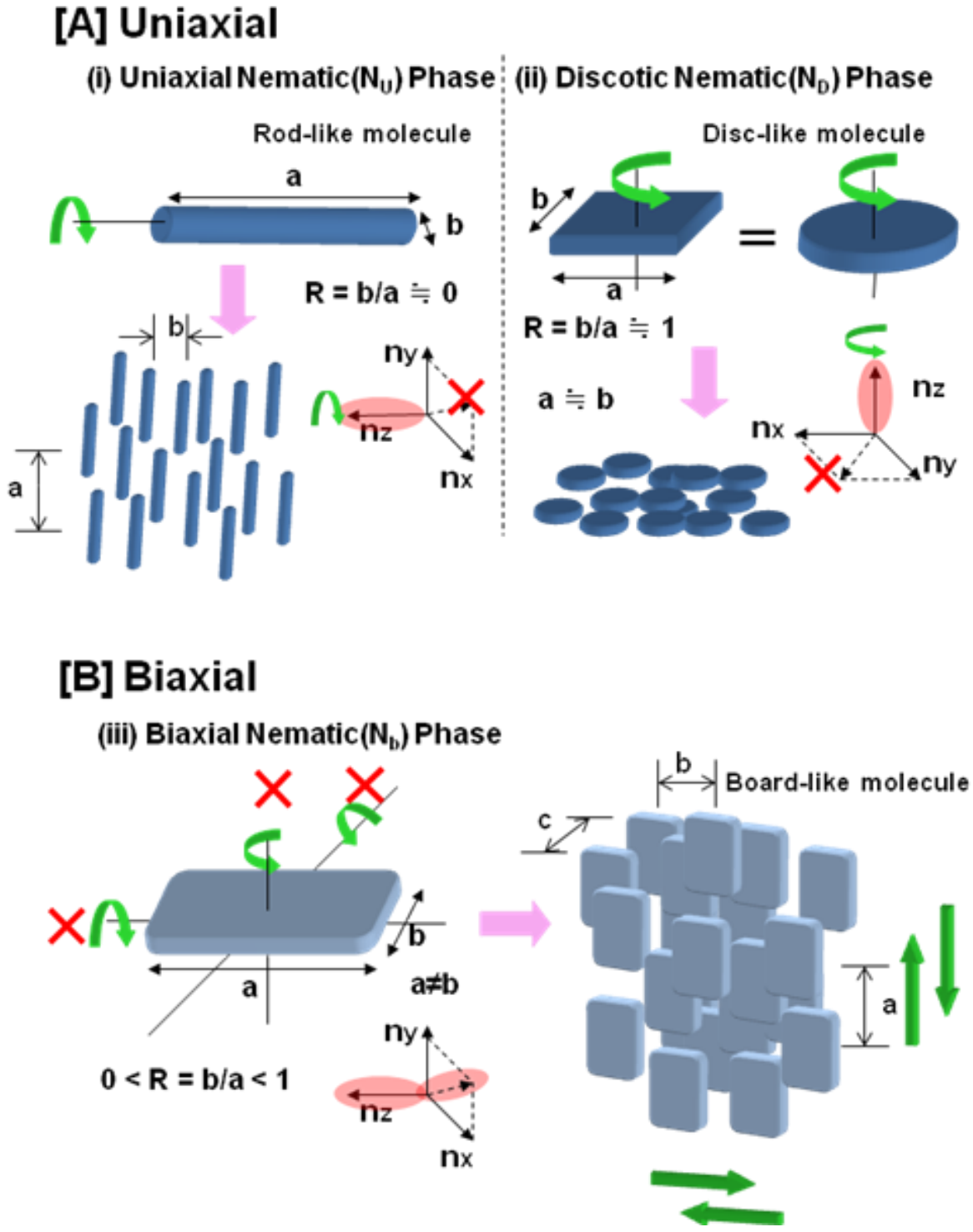

Fig. 1 Nematic mesophase structures.

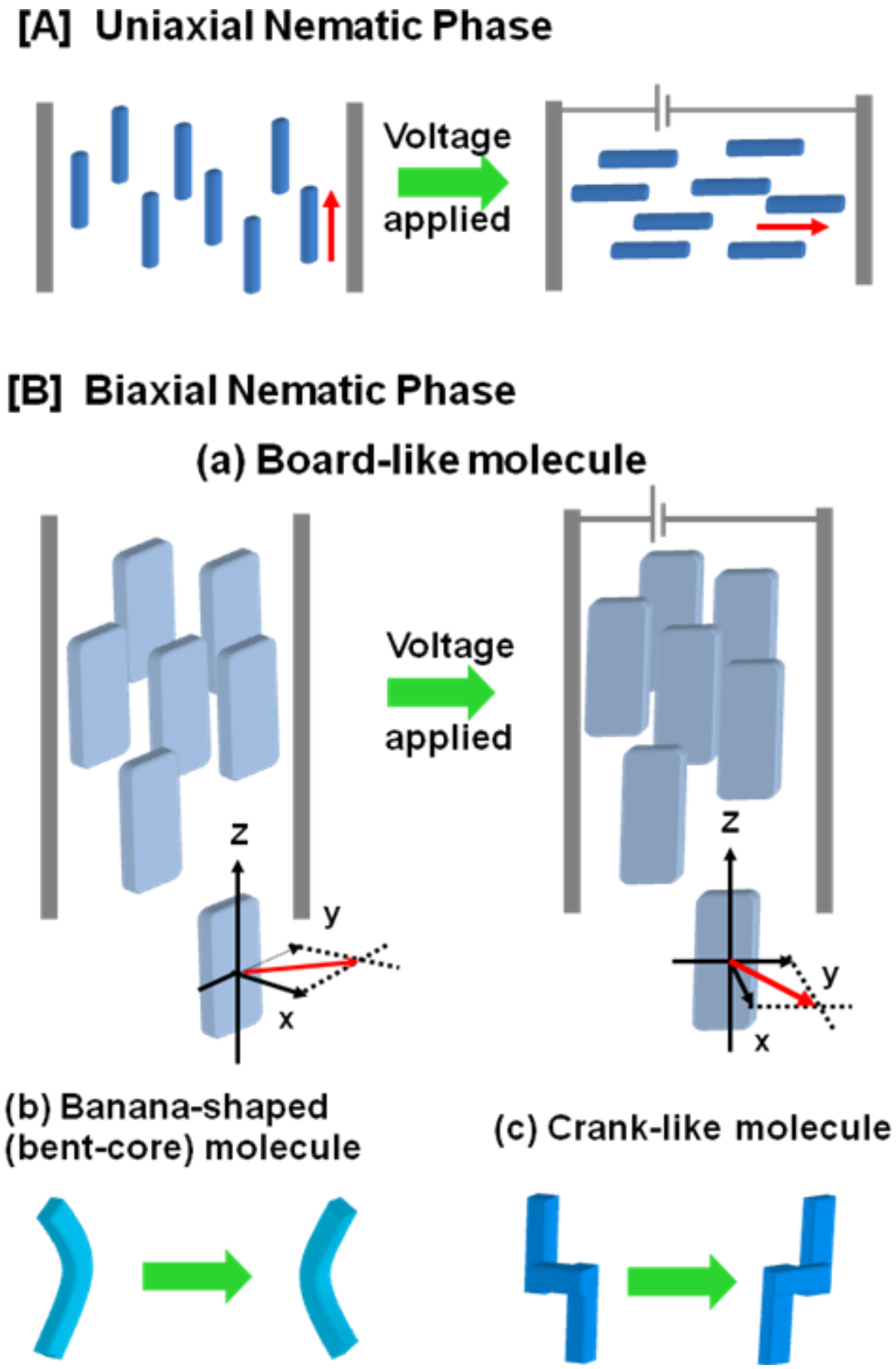

Fig. 2 Orientational changes of molecules by electric field [A] in a uniaxial nematic (N_u) phase and [B] in biaxial nematic (N_b) phases of (a) board-like molecules, (b) banana-shaped molecules and (c) crank-like molecules.

A: Chandrasekhar *et al.*

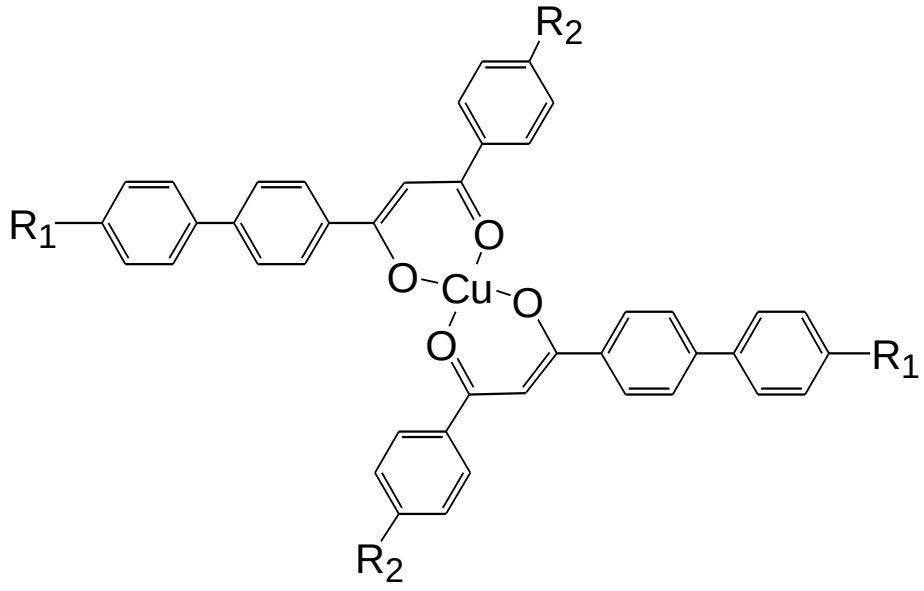

R_1=$C_{10}H_{21}$

R_2= CH_3, C_2H_5, CH_3O, C_2H_5O, C_3H_7O

Biaxial nematic phase ?

B: Our previous work

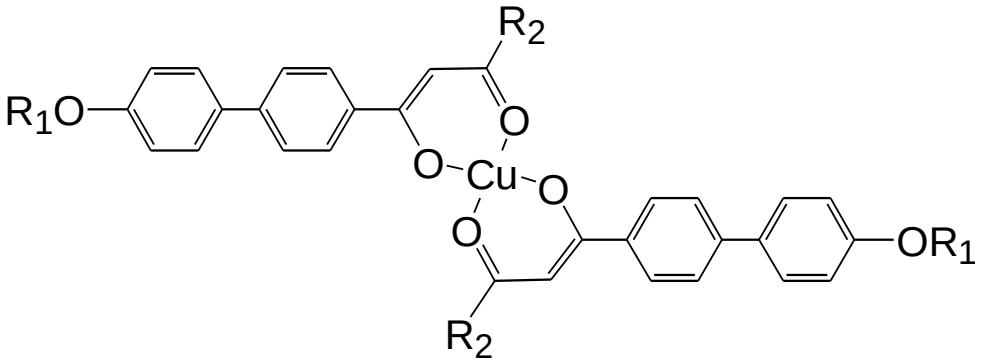

R_1=C_nH_{2n+1} (n = 6, 8, 10, 11, 12, 14)

R_2= C_2H_5

Optically positive uniaxial nematic phase

Fig. 3 Molecular formulae of the nematogens based on crank-like bis(ß-diketonato)copper(II) complexes, A and B.

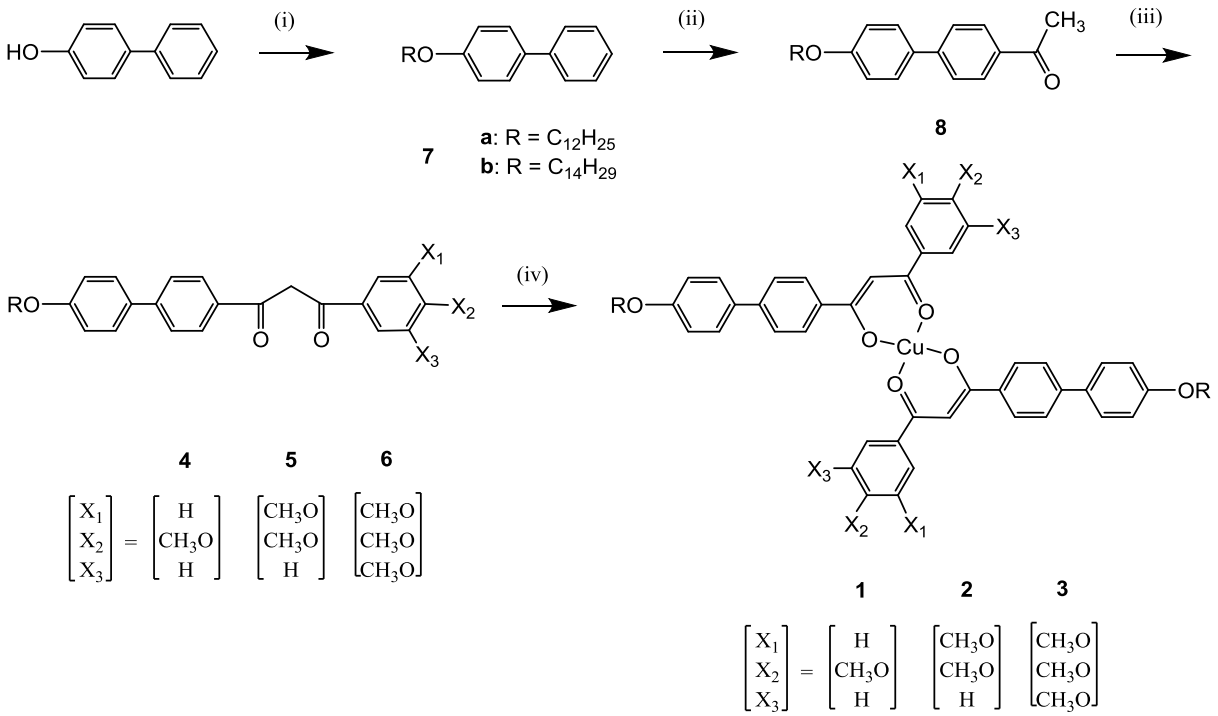

Scheme 1 Synthetic route for the novel bis(β-diketonato)copper(II) complexes, **1~3**, to obtain a biaxial nematic phase. (i) RBr, K_2CO_3 / DMF; (ii) CH_3COCl, $AlCl_3$ / CH_2Cl_2; (iii) (X_1, X_2, X_3)$PhCOOCH_3$, NaH/THF; (iv) $CuCl_2$, NH_4OH aq. sol /EtOH or KOH / toluene / ethyleneglycol.

Table 1 Elemantal analysis data of bis(β-diketonato)copper(II)complexes (**1~3**).

Compound	Mol. formula	Elemantal analysis; found(%) (calcd. %)	
		C	H
1a	$C_{68}H_{82}O_8Cu$	74.64 (74.87)	7.78 (7.58)
2a	$C_{70}H_{86}O_{10}Cu$	73.00 (73.05)	7.64 (7.53)
3a	$C_{72}H_{90}O_{10}Cu$	71.29 (71.41)	7.78 (7.49)
1b	$C_{72}H_{90}O_8Cu$	75.67 (75.39)	8.03 (7.91)
2b	$C_{74}H_{94}O_{10}Cu$	73.52 (73.63)	8.10 (7.85)
3b	$C_{76}H_{98}O_{12}Cu$	72.30 (72.04)	7.95 (7.80)

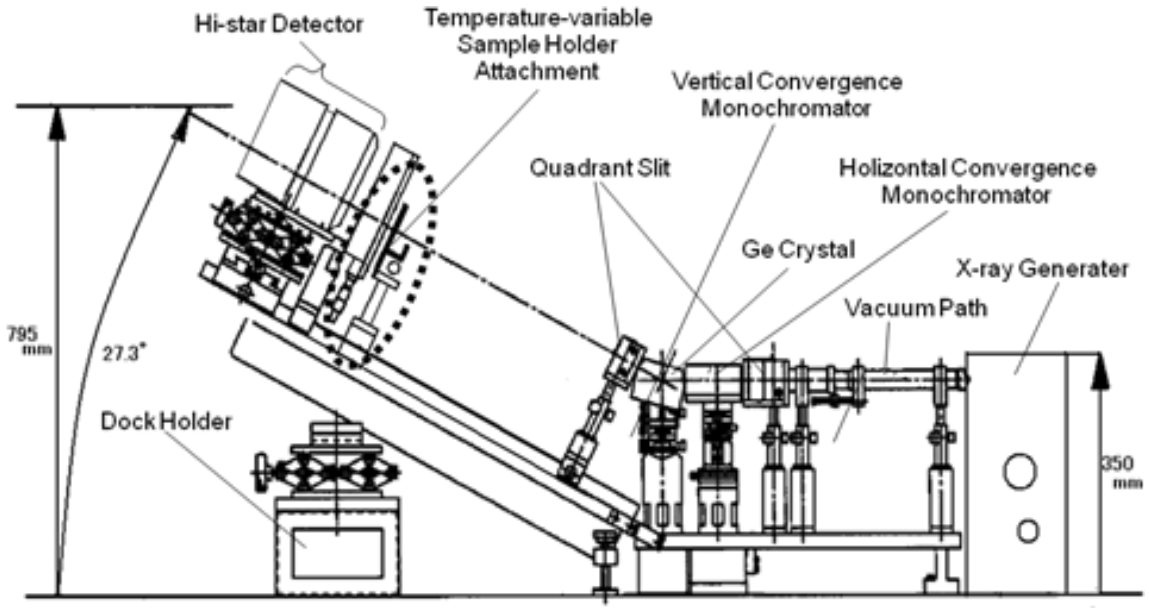

Fig. 4 Setup of small-angle X-ray scattering (Bruker MAC SAXS) equipped with a temperature-variable sample holder.

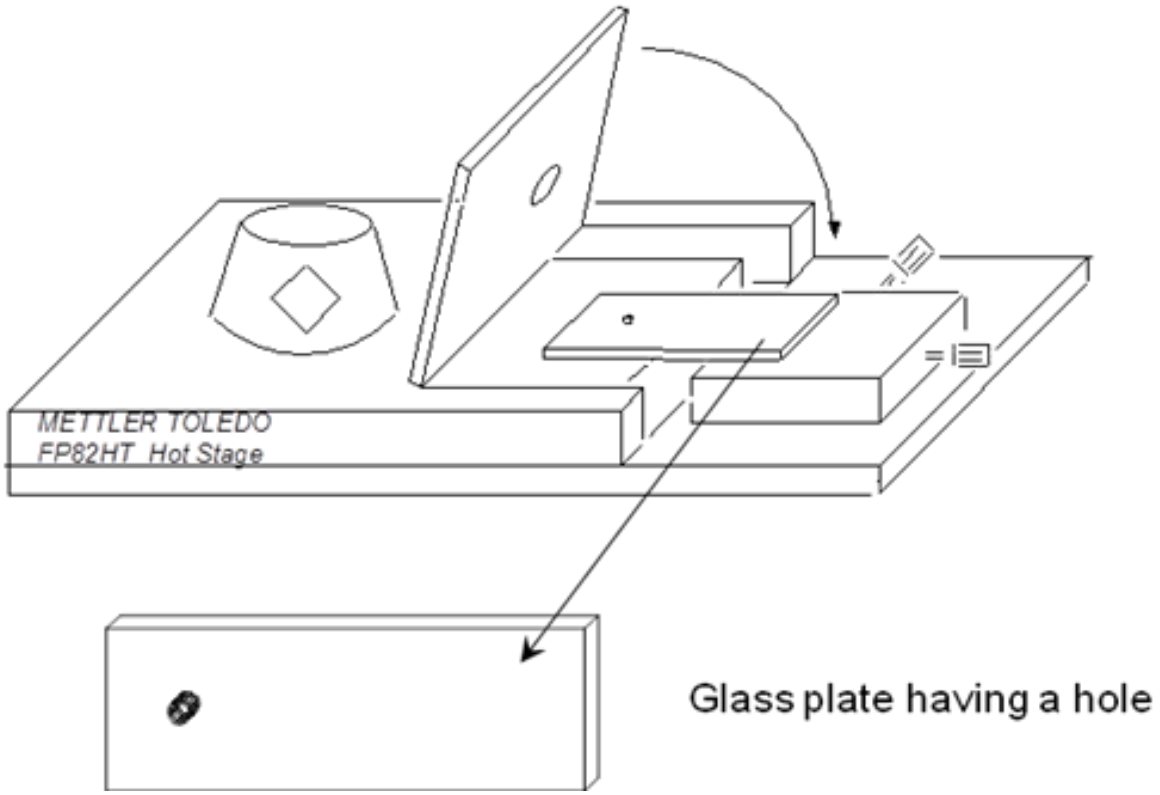

Fig. 5 Setup of the temperature-variable sample holder.

Table 2 Phase transition temperatures and enthalpy changes of the ligands **4~6** and the copper complexes **1~3**.

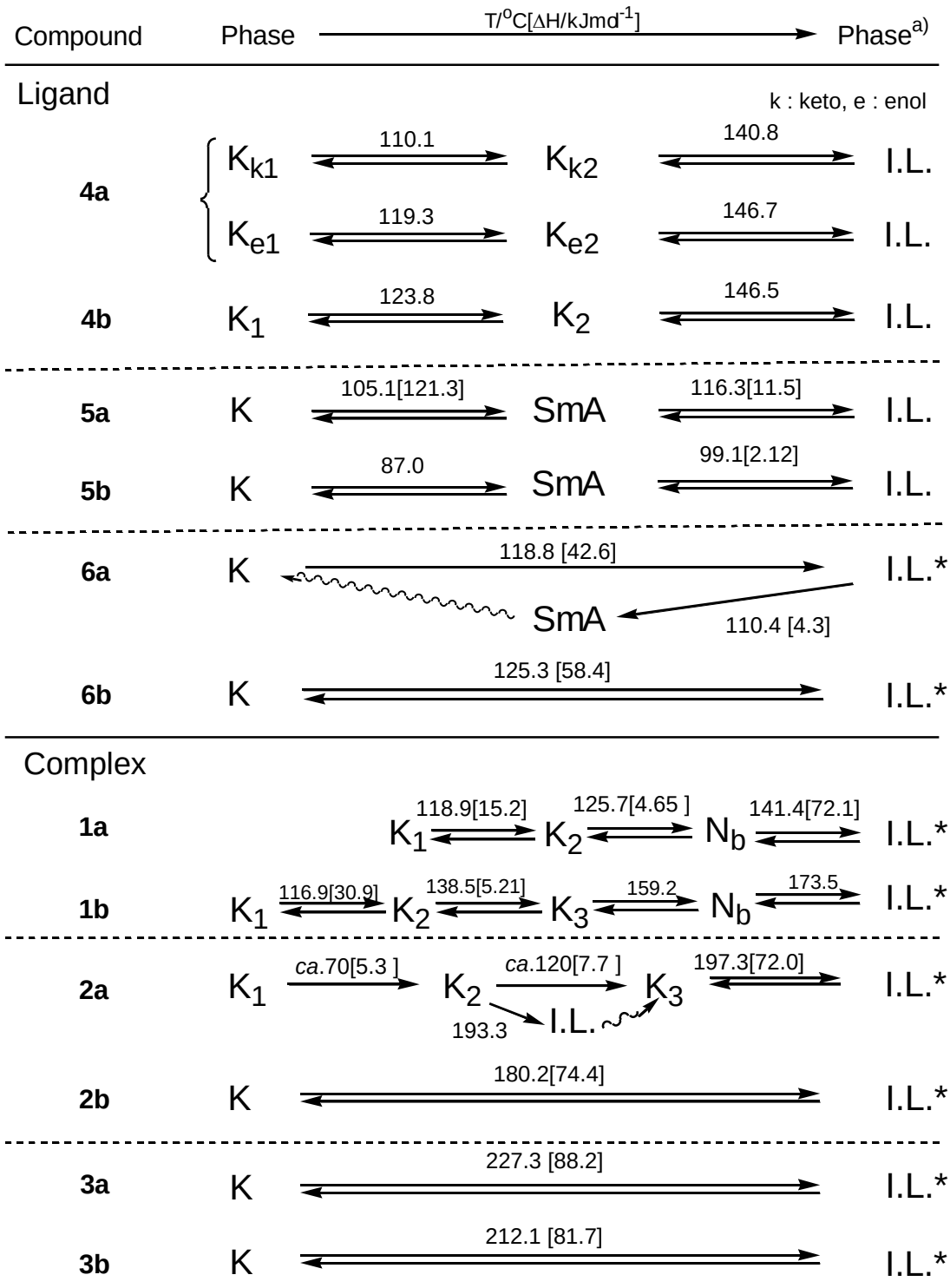

a) Phase nomenclature: K = crystal, N_b = biaxial nematic phase, SmA = smectic A phase, I.L. = isotropic liquid and *= gradually decomposition. a) Phase nomenclature: K = crystal, Nb = biaxial nematic phase, SmA = smectic A phase, I.L. = isotropic liquid and *= gradually decomposition. K_{k1} and K_{k2} represent crystalline phases in the keto form. $K_{e1}$and K_{e2} correspond to crystalline phases in the enol form.

[A]

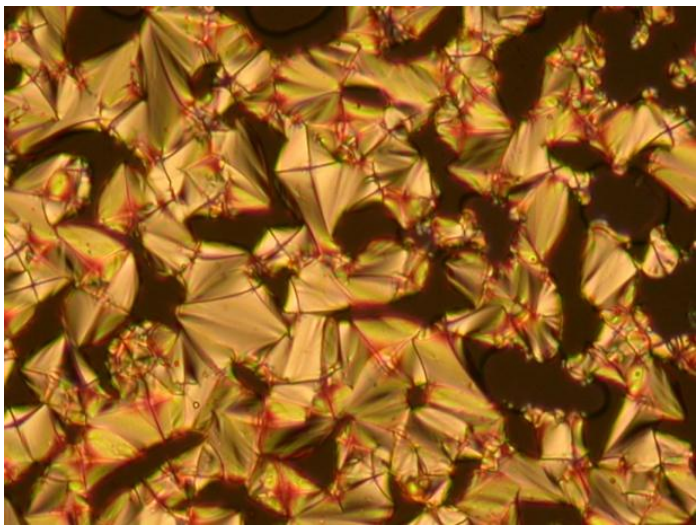

[B]

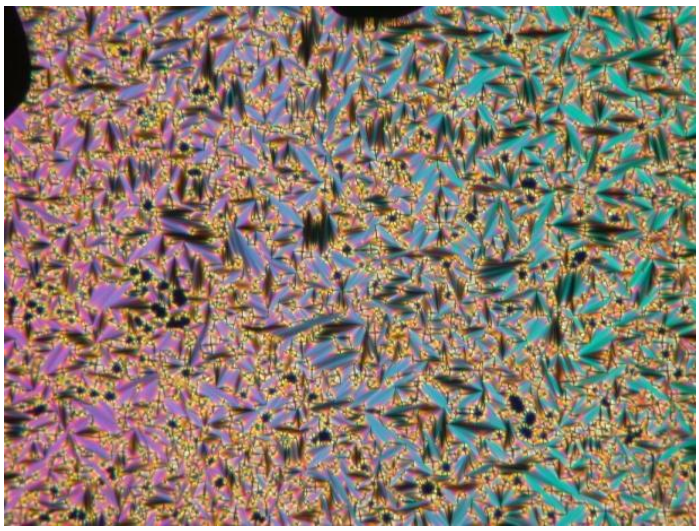

[C]

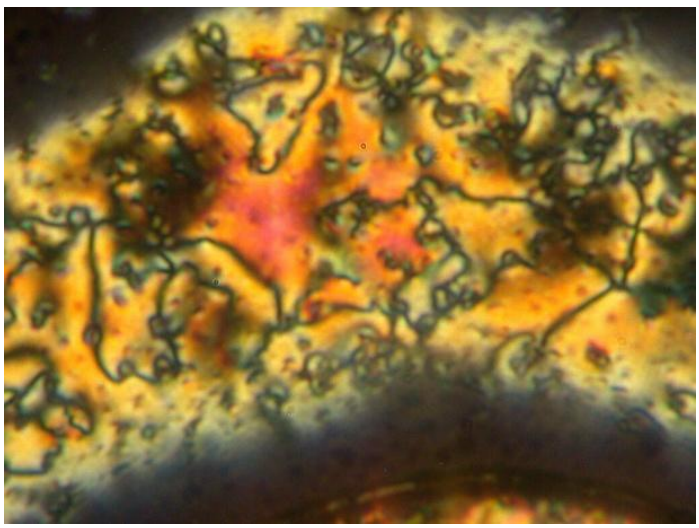

Fig. 6 Photomicrographs of [A] **6a** at 111.2 °C, [B] **5a** at 114.3 °C, and [C] **1a** at 137.7 °C.

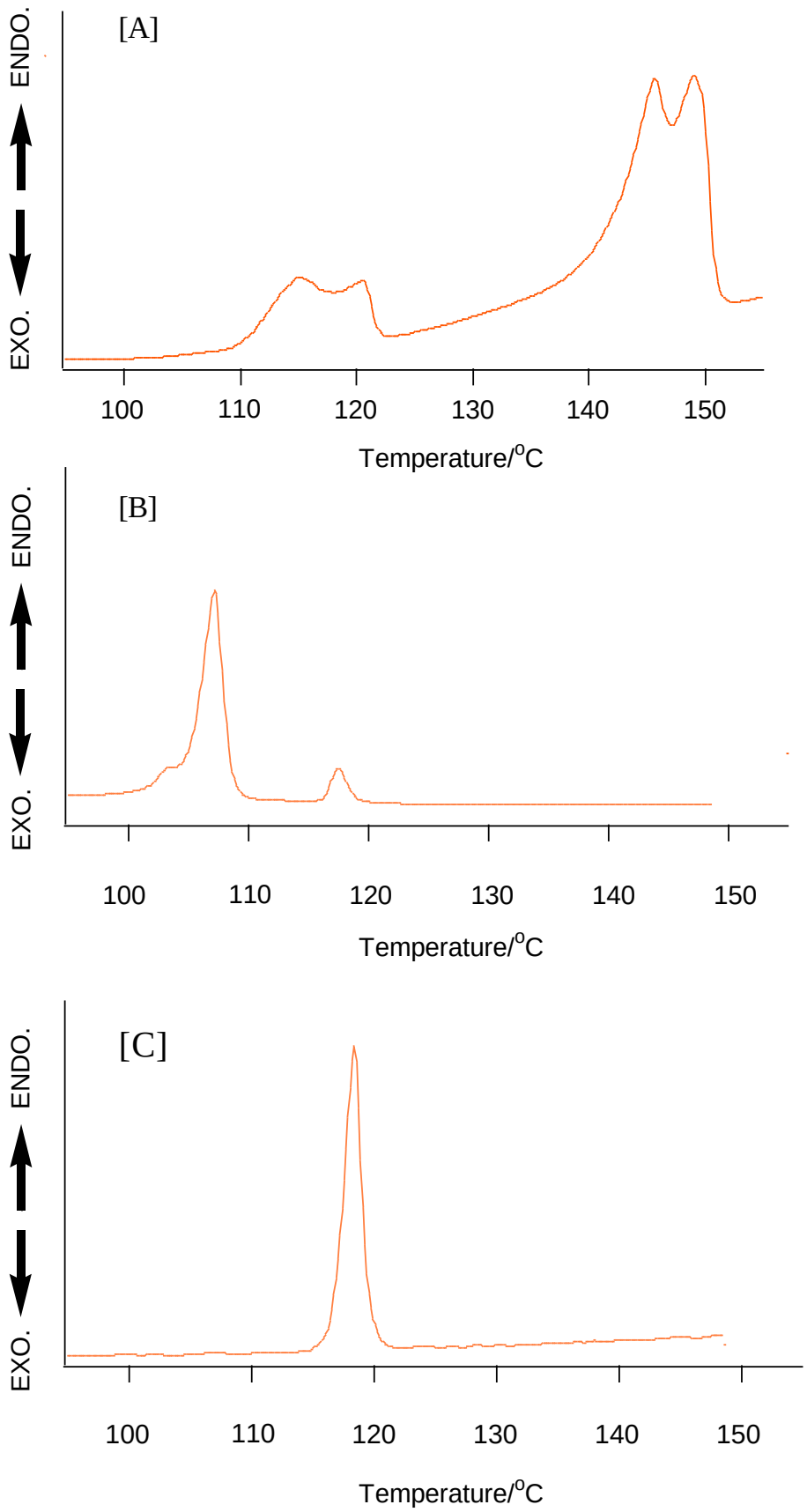

Fig. 7 DSC thermograms of the ligands: [A] **4a**, [B] **5a** and [C] **6a** at 10.0 ^{o}Cmin^{-1}.

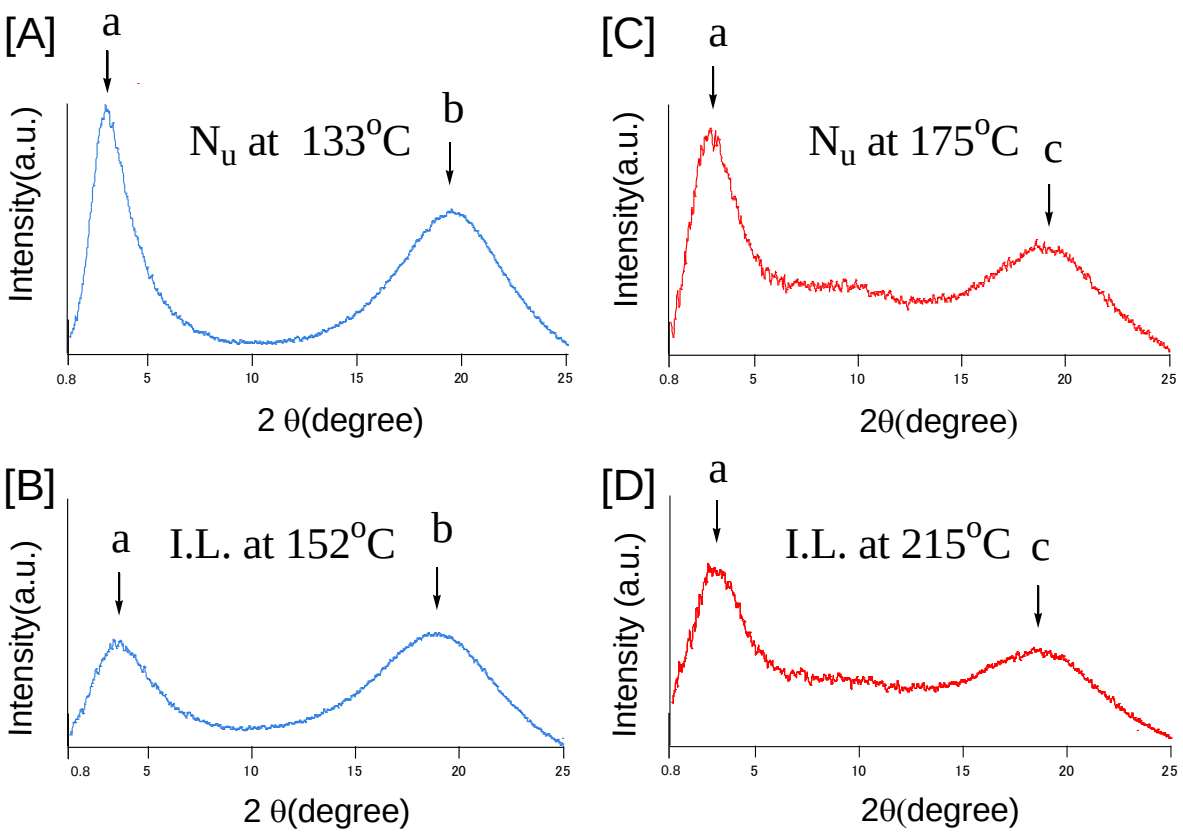

Fig. 8 X-ray diffraction patterns of [A] N_u at 133 °C and [B] I.L.at 152 °C for p-n-decyloxybenzoic acid; [C] N_u at 175 °C and [D] I.L. at 215 °C for bis[1-(4-dodecyloxybiphenyl)-3-ethylpropane-1,3-dionato]copper(II) complex. The arrows a and b in [A] and [B] correspond to the average distances a and b illustrated in Fig. 1[A](i), respectively. The arrows a and c in [C] and [D] correspond to the average distances a and c illustrated in Fig. 1[B](iii), respectively.

Table 3 X-ray data of the various nematic phases of *p-n*-dodecyloxy-benzoic acid, bis[1-(4'-dodecyloxybiphenyl)-3-ethyl-propane-1,3-dionato]copper(II), **1a** and **1b**.

Compound (mesophase) Lattice constants/Å	Peak No.	Spacing/Å Observed	Spacing/Å Calculated	Miller indices (*h k l*)
p-n-Dodecyloxybenzoic acid				
N_u at 133°C	1	29.90	29.90	(1 0 0)
a = 29.90 c = 4.54	2	4.54	4.54	(0 0 1)
Z = 1.0 for ρ = 1.0				
Bis[1- (4'-dodecyloxybiphenyl)-3-ethyl-propane-1,3-dionato]copper(II)				
N_u at 175°C	1	30.47	30.47	(1 0 0)
a = 30.47 c = 4.64	2	4.64	4.64	(0 0 1)
1a				
N_b at 136°C	1	35.64	35.64	(1 0 0)
a = 35.61 b = 21.34 c = 4.64	2	21.34	21.34	(0 1 0)
Z = 2.0 for ρ = 1.0	3	4.64	4.64	(0 0 1)
1b				
N_b at 164°C	1	33.85	33.85	(1 0 0)
a = 33.85 b = 23.88 c = 4.85	2	23.88	23.88	(0 1 0)
Z = 2.1 for ρ = 1.0	3	4.85	4.85	(0 0 1)

ρ: Assumed density (g/cm^3).

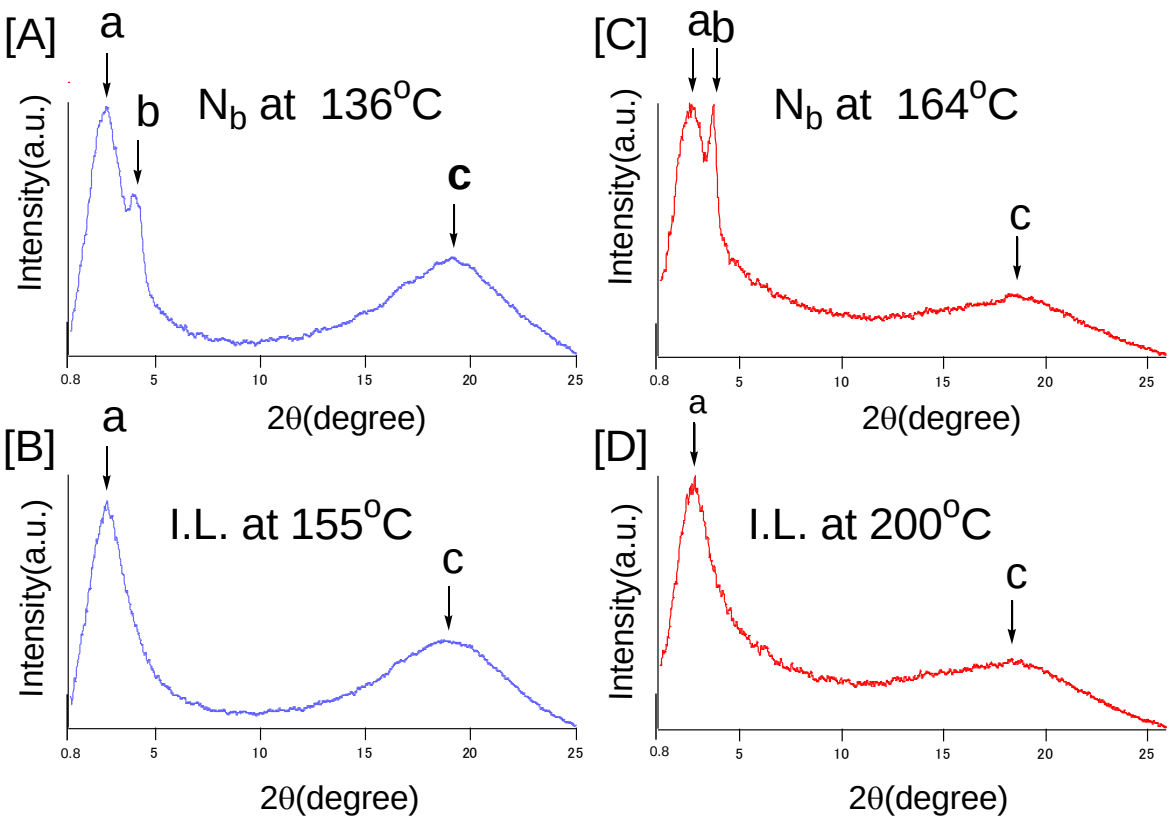

Fig. 9 X-ray diffraction patterns of [A] N_b at 136 °C and [B] I.L. at 155 °C for bis[1-(4'-dodecyloxybiphenyl)-3-(4-methoxy-phenyl)propane-1,3-dionato]copper(II) (**1a**); [C] N_b at 164 °C and [D] I.L. at 200 °C for bis[1-(4'-tetradecyloxybiphenyl)-3-(4-methoxyphenyl)-propane-1,3-dionato]copper(II) (**1b**). Arrows a, b and c in this figure correspond to the average distances a, b and c illustrated in Fig. 1[B](iii), respectively.

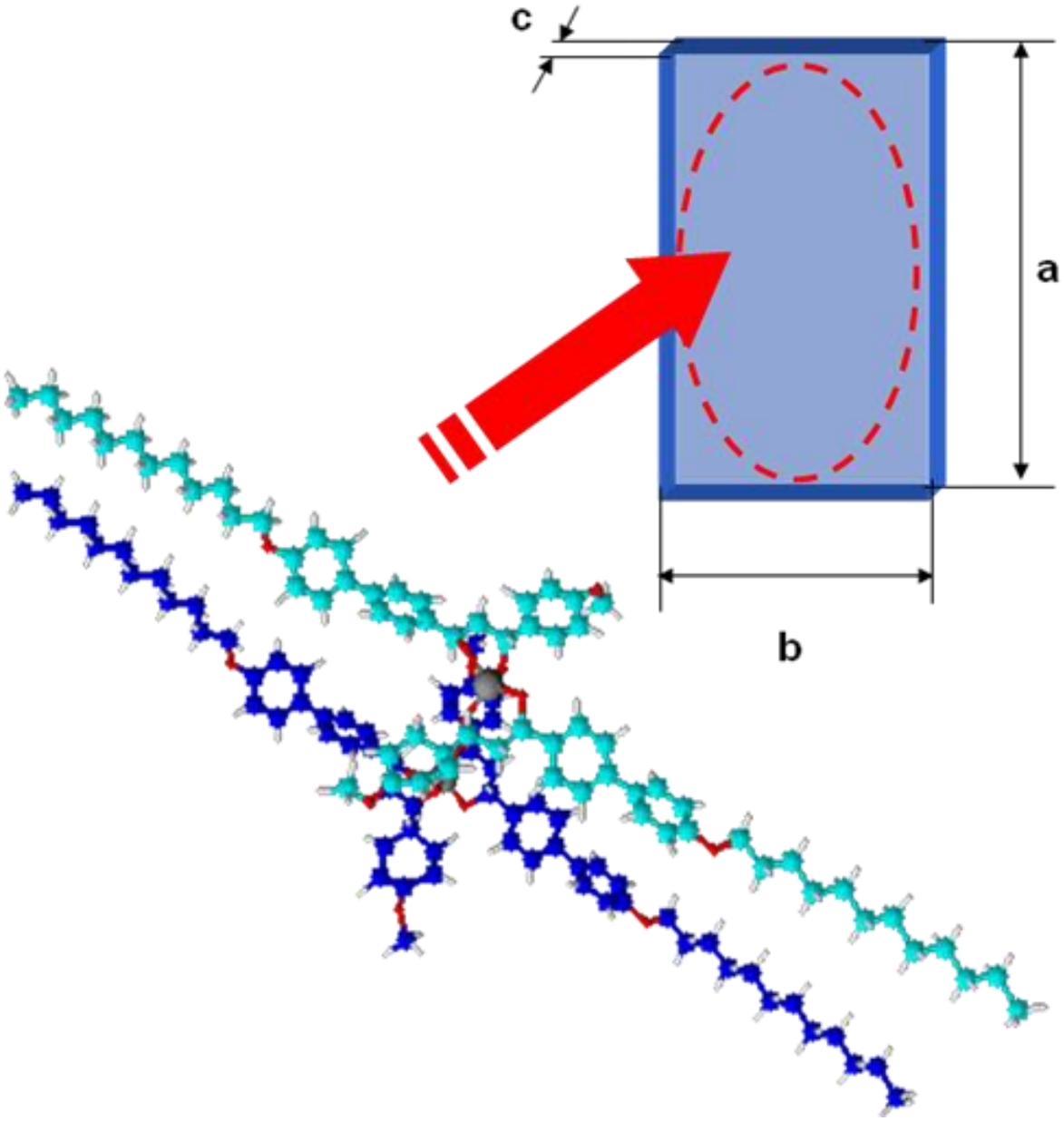

Fig. 10 Proposed rectangular parallelepiped dimer model for **1a** and **1b** in the N_b phase. The sizes a, b and c of the rectangular parallelepiped dimer in this figure correspond to the average distances a, b and c illustrated in Fig. 1[B](iii), respectively. The present values, a, b and c, were obtained from the XRD studies shown in Fig. 9.